Molecular Vision 3: 6, 1997 <http://www.emory.edu/molvis/v3/kolb>
Received 2 Feb 1997 | Accepted 23 Apr 1997 | Published 10 June 1997

Neural circuitry and light responses of the dopamine amacrine cell of the turtle retina

H. Kolb[1*], E. Netzer[1], and J. Ammermüller[2]

[1]John Moran Eye Center, University of Utah Health Sciences Center, Salt Lake City, Utah, U.S.A. and the [2]Department of Neurobiology, University of Oldenburg, Oldenburg, Germany

Purpose: To understand the circuitry and electrophysiology of the dopamine cells in the turtle retina.

Methods: Preembedding immunocytochemistry for tyrosine hydroxylase (Toh) was done on vibratome sections of turtle retina. Resultant Toh-immunoreactive (Toh-IR) amacrine cells were then serially thin-sectioned for analysis by electron microscopy (EM). Some sections of Toh-IR cells also were post-embedding immunostained for glycine and GABA content. Intracellular recordings and dye markings were made from the turtle eyecup and slice preparation to determine the light responses of cells called A28, which have the same morphology as Toh-IR amacrine cells.

Results: Physiologically A28 cells were L-type (luminosity) and gave sustained depolarizing (ON center) responses to light pulses. High intensity light pulses produced immediate transients and long depolarizations, lasting beyond the stimulus duration. An after-hyperpolarization and an antagonistic surround could be elicited. EM reconstruction of a Toh-IR cell revealed new circuitry over that described before (**Pollard, J. & Eldred, W.D. (1990) J. Neurocytol. 19, 53-66**). Bipolar ribbon synapses occurred in all three dendritic tiers. However, amacrine cell inputs dominated numerically (95% amacrine input, 5% bipolar input) many of them in a serial synaptic configuration. GABA+ inputs were seen but not glycine+ inputs. Output from Toh-IR profiles was primarily to large ganglion cell dendrites but also to bipolar cell axons, GABA-IR amacrines, unspecified amacrine cells and other Toh-IR dendrites.

Conclusions: The synaptology of the dopamine cells of the turtle retina suggests that sustained inhibitory amacrine cell pathways, including GABAergic pathways, are chiefly responsible for their response characteristics at low light levels. Conversely, at higher light intensities, transient excitatory amacrine cells probably have influence.

In the turtle retina, Toh-IR amacrine cells are medium-field sized, tristratified amacrine cell types (1-4). They are called A28 because of their morphological resemblance to Golgi-impregnated amacrines named A28 cells (5) that have similar branching patterns and stratification levels. The dendrites of turtle Toh-IR amacrine cells form a dense plexus in stratum 1 of the IPL, as in other species, but they also have two other tiers of dendrites branching in the strata 2/3 and 4/5 borders. A previous EM study of turtle Toh-IR cell connectivity (1) provided initial data on synaptic input density and general connectivity. Since then, new information concerning the physiology and laminar organization of the bipolar, amacrine, and ganglion cells that might have input to this cell type in turtle retina has become available (6-10). We thought it worthwhile to repeat a synaptic analysis and correlate it with new and past intracellular recordings (6). We hope herein to provide a richer interpretation of the role of such cells in the turtle retina in particular, and in the vertebrate retina in general.

MATERIALS AND METHODS

Pre-embedding procedures—Young adult turtle (Pseudemys scripta elegans) retinas were fixed flat between filter paper in 2% formaldehyde and 0.5% glutaraldehyde for 2 hrs before transferring to an overnight fixation in 4% paraformaldehyde in PBS with 0.1 M $NaHCO_3$ (pH 10.4). The following day the retinas were put through a freeze-thaw procedure (11) after which they were washed in PBS and sectioned into 50 µm vertical slices on a vibratome. After incubation in 10% normal goat serum for 1 hr at 4˚C they were placed in the primary antibody, rabbit-anti-Toh (Eugene Tech) at a concentration of 1:500 in PBS for 4 days at 4˚C. After further washes in PBS the tissue was transferred to biotinylated goat anti-rabbit IgG diluted 1:100 in PBS for 2 days at 4˚C. More washes in PBS occurred before transfer to a solution of the ABC (avidin-biotin complex) in 0.1M PBS for two days. Finally, the retinas were washed and incubated in 3,3-diaminobenzidine tetrahydrochloride (DAB), with 0.01% H_2O_2 for 15 min. Subsequently, the slices of retina were post-fixed in 1% OsO_4 in 0.1M PBS for 1 hr, and processed for plastic embedding and serial thin sectioning for electron microscopy (34).

Post-embedding immunostaining of ultrathin sections—Some of the EM thin sections were processed for post embedding immunocytochemistry as described in previous work from our laboratory (34). Incubation was in rabbit anti-GABA conjugated with 1% bovine serum albumin (BSA) (Chemicon) diluted 1:500 or rabbit-anti-glycine (Chemicon) used at various concentrations (1:40, 1:80, 1:160 and 1:320) + 0.5% Triton in TBS for 1 hr on a shaker at room temperature. Incubation took place in the secondary antibody of anti-rabbit IgG conjugated with gold particles (15 nm) (Janssen/Amersham) diluted 1:20 for GABA and 1:20 or 1:40 for glycine in TBS + 1% BSA + 0.5% Triton for 1 hr on a shaker at room temperature.

We analyzed large montages of GABA or glycine stained sections in order to determine significant staining of inner nuclear layer cell bodies over background. For the GABA data, we accepted only stained profiles in tissue where the "hot" cells labelled 8X or better over the background while for

*To whom correspondence should be addressed: Dr. Helga Kolb, John Moran Eye Center,University of Utah Health Sciences Center, 50 N. Medical Drive, Salt Lake City, Utah 84132, U.S.A., phone: 801-585-6510, fax: 801-581-3357 e-mail: hkolb@msscc.med.utah.edu

glycine we accepted profiles labeling 9X over background (34). The images of neuropil containing colloidal gold showing GABA, for example, were always followed through 5 or 6 serial sections (all sections of the grid) and profiles were considered labeled when there were a consistent 4 -6 particles of gold present compared with neighboring, unlabeled profiles with next to no particles through the series.

Electrophysiology—Intracellular recordings and staining with HRP-filled microelectrodes were done on an everted eye-cup preparation as described in detail in Ammermüller and Kolb (6). The light stimulation protocols were the same as in previous papers (6, 7). After recording and HRP injection A28-like amacrine cells were processed for HRP histochemistry (6). Stained cells were drawn by camera lucida to reveal their branching patterns and to make a careful assessment of their stratification level within the IPL. Some recordings were performed in a retinal slice preparation. The preparation procedure closely followed that of Burkhardt et al. (12). Exact stimulus parameters are indicated in the figure legends.

RESULTS

Light microscopy of Toh-IR amacrine cells— The amacrine cell type that was immunocytochemically stained with antibodies to tyrosine-hydroxylase (Toh-IR) has the appearance described before (1-4) of a medium-field, tristratified amacrine, classified as A28 (5) (Figs. 1a, 5a). It is characterized by a medium cell body (10 x 12 µm) and 300-500 µm diameter dendritic field consisting of very fine diameter, curvy, multibranched dendrites bearing appendages and terminals (Fig. 1a). A plexus of dendrites lies in strata 1 of the IPL under the amacrine cell bodies at the inner nuclear layer (INL) IPL border while two other, well-defined plexi branch loosely on approximately the 2/3 and 4/5 borders of the IPL (Fig. 1b).

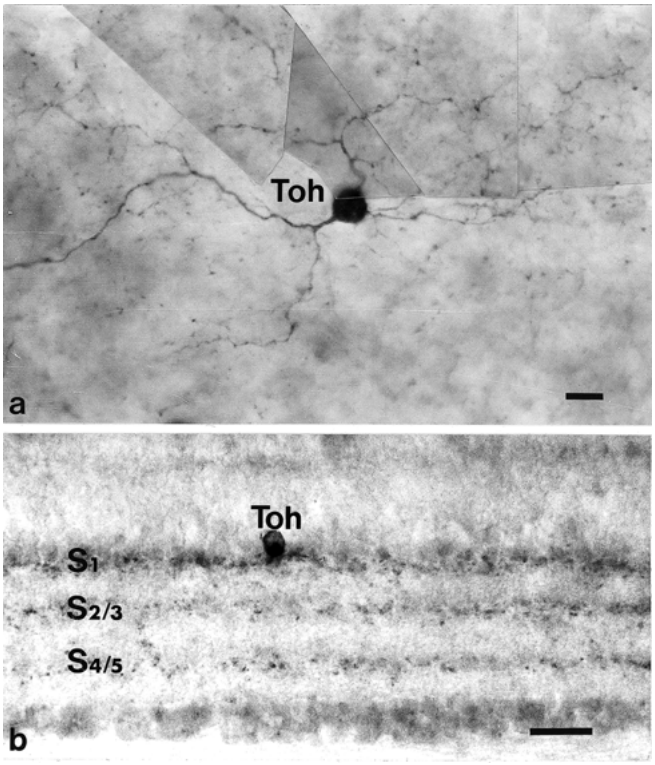

Figure 1a. LM view of a wholemount Toh-IR cell. LM view of a wholemount Toh-IR cell. Scale bar 10 µm. Figure 1b. Vibratome vertical section of Toh-IR amacrine cell. Vibratome vertical section of Toh-IR amacrine cell. The dendrites clearly form three tiers of branches in stratum 1 (S1), S2/3 and S4/5 of the IPL. Scale bar 25 µm.

We could find no evidence for any Toh-IR processes or HRP-injected processes originating from such amacrine cells in either the INL or the OPL, so they do not appear to be interplexiform cells in the turtle retina. Nor have we seen evidence of putative dopamine amacrine cells of turtle having "axon-like" processes as has been seen for dopamine amacrine cells in cat and primate retinas (13,14).

Electron microscopy of Toh-IR amacrine cells— We performed an EM study on three Toh-IR amacrine cells taken from 20 µm thick radial sections. One of these cells was rather completely reconstructed, allowing us to look at the entire cell body and major dendrites in 150 µm wide and 60 µm depth of the IPL neuropil (cell reconstructed in Fig. 4). Figures 2 and 3

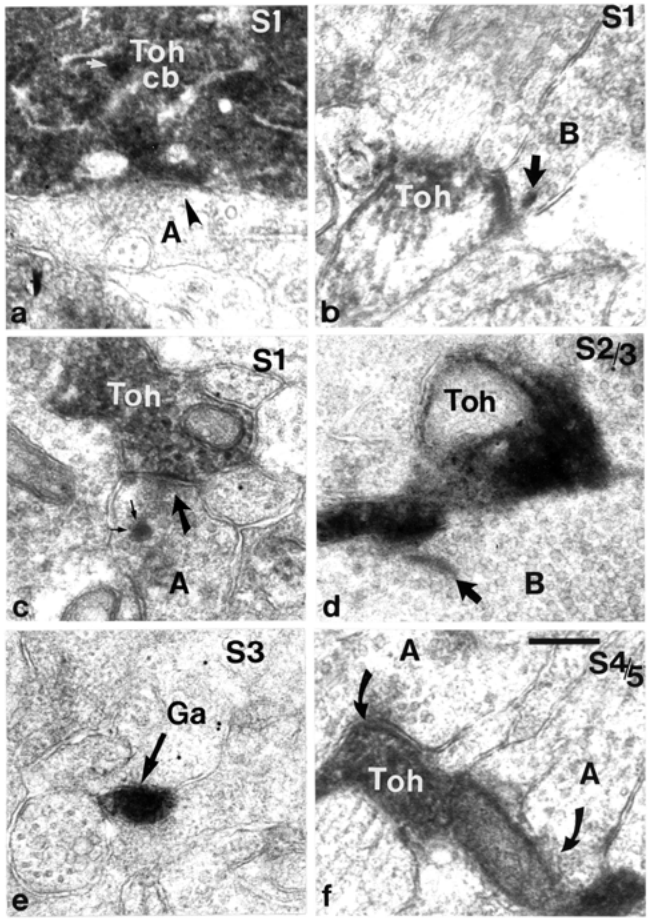

Figure 2. **a)** An amacrine profile (A) makes a narrow-cleft synapse with small caliber synaptic vesicles (arrowhead) upon the base of the Toh-IR cell body in stratum 1 of the IPL. The Toh-IR cell cytoplasm contains dense-cored vesicles (white arrow). **b)** Bipolar (B) ribbon input (arrow) to a Toh-IR profile in S1 of the IPL. **c)** A dense-cored vesicle (fine arrows) containing amacrine profile (A) is presynaptic (large arrow) to a Toh-IR process in S1 of the IPL. **d)** A bipolar cell profile (B) is presynaptic (arrow) to a Toh-IR profile in S2/3. **e)** A GABA+ amacrine (Ga), containing colloidal gold particles, is presynaptic to a small Toh-IR profile in S3. **f)** Two wide-cleft synapses from amacrine cells (A, curved arrows) upon a Toh-IR process in S4/5. Scale bar for all 0.5 µm.

show example micrographs of synaptic input and output to and from the Toh-IR cell.

Bipolar ribbon synapses occurred to both large and small diameter Toh-IR dendrites in all three tiers of dendrites (Fig. 2b and d, arrow points to bipolar ribbon). These ribbon synapses came from bipolar axons in both stratum 1 and strata 2/3 and 4/5 borders. In some instances we could also see Toh-IR profiles making synapses upon bipolar axons particularly in stratum 1. Amacrine cell synapses were very numerous on the cell body (Fig 2a) and over all the dendrites in all three tiers of dendrites (Figs. 2c and f). Some cytological characteristics distinguished one amacrine cell from another. For example, many of the presynaptic amacrine profiles were of large diameter, electron lucent, and had very distinct, large clusters of synaptic vesicles at presynaptic membranes of wide-cleft synapses (Fig. 2f, curved arrows). Other amacrine profiles were smaller in diameter, with small synaptic vesicles and little or no enlargement of the synaptic cleft (Fig. 2a, arrowhead). Many of the presynaptic amacrine profiles contained dense-cored vesicles (Fig. 2c, two fine arrows). Dense cored vesicles were also present in the Toh-IR cell body itself and major dendrites (Fig. 2a, white arrow). Stratum 1 of the IPL was particularly dense in Toh-IR dendrites making and receiving amacrine synapses and many amacrines were in serial synaptic arrangements (Fig. 2f, curved arrows).

A small number of sections were postembedding labeled to determine whether glycine or GABA was present in pre- and postsynaptic amacrine profiles. We found only GABA-containing amacrines to be involved with the Toh-IR dendrites (Fig. 2e, Ga, arrow). GABA-IR amacrine synapses were seen upon Toh-IR dendrites in strata 1 and 3 but since the sample was small we cannot rule out such input to the other levels of stratification.

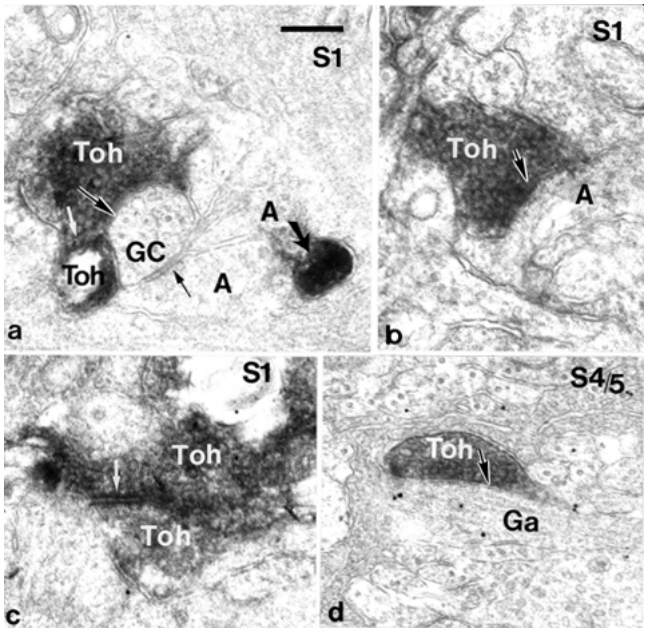

Figure 3. EM of Toh-IR amacrine cells: Toh-IR profiles presynaptic to bipolar axons, ganglion cell dendrites and amacrine cell profiles. **a)** Toh-IR processes are presynaptic to other Toh-IR processes (white arrow) and to a ganglion cell (GC) dendrite (black/white arrow) in S1. The GC dendrite is also postsynaptic to an unstained amacrine cell (A). A neighboring unstained amacrine cell (A) is presynaptic to another Toh-IR process. **b)** A vesicle-filled Toh-IR process is presynaptic (black/white arrow) to an unstained amacrine cell (A) in S1 of the IPL. **c)** A large Toh-IR process makes a synapse upon another smaller Toh-IR profile in S1. **d)** A Toh-IR profile on the S4/5 border synapses upon a colloidal gold-containing GABA-IR (Ga) amacrine profile. Scale bar 0.5 µm.

Synaptic output from Toh-IR dendrites to postsynaptic profiles were often difficult to discern because of the immunostain density. However, we have evidence for Toh-IR profiles presynaptic to bipolar axons, ganglion cell dendrites (Fig. 3a, black and white arrow) and amacrine cell profiles (Fig. 3b, black and white arrow) at all stratification levels of the Toh cell's dendritic tree. Some of the amacrines proved to be GABA-IR profiles (Fig. 3d, black and white arrows, Ga). Toh-IR dendrites frequently engaged in synapses between themselves as shown in Figures 3a and c (white arrows).

Summary and quantitation of synapses upon the Toh-IR amacrine cell— A summary drawing showing the Toh-IR cell body and its major dendrites running in stratum 1 and passing down to the strata 2/3 and 4/5 borders is shown in Figure 4. All of the synaptic arrangements that could be positively identified in the serial section analysis are indicated on the drawing and in Table 1. The pre- or postsynaptic GABA-IR profiles are indicated in the drawing (Fig. 4) but their number are not quantifiable relative to the other numbers, because only a limited number of postembedded stained sections were available for study.

This Toh-IR cell type received primarily amacrine cell inputs (Fig. 4, red squares) but also a few bipolar cell ribbon synapses (Fig. 4, green squares) (95% amacrine input, 5% bipolar input, Table 1). The amacrine inputs seemed scattered throughout the five strata of the IPL while the bipolar inputs were concentrated to the three tiers of dendrites. Clearly the tier of dendrites in stratum 1, where the thickest plexus of

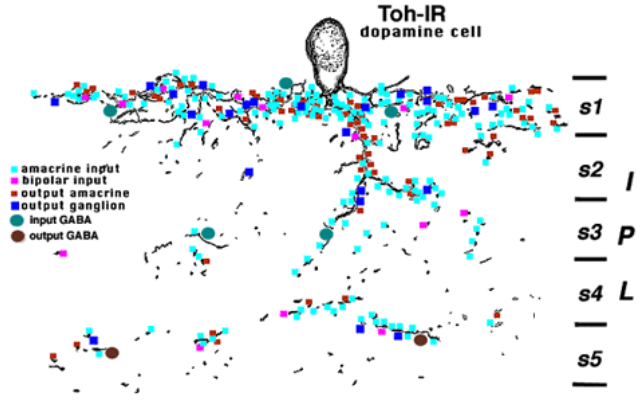

Figure 4. Reconstruction of a Toh-IR cell body and main dendrites in S1 and passing to S2/3 and S4/5. Other Toh-IR dendrites in the tissue were studied but did not necessarily get traced to the Toh-IR cell body. In the 15 µm thick slab of tissue studied by EM, the Toh-IR cell and related processes received mostly amacrine synapses (red) in all strata of the IPL, and a few bipolar ribbon synapses (green) to the main tiers of dendrites in stratum 1, strata 2/3 and 4/5 borders. Toh-IR stained profiles were presynaptic to amacrine and ganglion cell processes (blue, yellow). Postsynaptic ganglion cell dendrites costratified in the three main dendritic tiers of the Toh-IR cell.

overlapping Toh-IR dendrites is found, is most heavily laden with all types of synaptic inputs and outputs (Fig. 4). Output from Toh-IR profiles was to large ganglion cell dendrites (Fig. 4, yellow squares) (Table 1, 30% output to ganglion cells) and like the bipolar inputs, occurred rather strictly in the three tiers of dendrites. The numerically superior output to amacrine cells (Table 1, 60% output to amacrine cells) occurred mostly in stratum 1 but also throughout all the IPL neuropils (Fig. 4, blue squares). Toh-IR dendrites synapse amongst themselves en passant particularly in stratum 1 (Table 1, 10% Toh to Toh cells) (not illustrated in Fig. 4). We noted a few synapses from the Toh-IR cell to bipolar cell axon terminals (Table 1, 1% output to bipolar cells).

Intracellular recordings from A28 cells that have the same morphology as Toh-IR amacrine cells— Three HRP-filled, tristratified, medium-field amacrine cells, called A28 cells, with the morphology of the Toh-IR amacrine cell of the turtle retina, were intracellularly recorded and dye-injected (6). The three cells gave the same general types of responses to light spots or slits of different sizes, intensities, annuli and color, although they varied slightly in details of response shapes.

Figure 5 shows the morphology of one of the HRP-injected A28 cells recorded from a slice preparation of turtle retina and its intracellular responses to light of different shapes, intensities, and wavelengths. Receptive field center stimulation with slits of white light of increasing width produced sustained depolarizations (Fig. 5b). The black bar and the widest slit brought in some surround inhibition indicative of a center surround receptive field organization. Stimulation with red, green or blue light produced the same signed ON center responses, although red light was the most efficient (Fig. 5c). All three A28 cells that we have recorded over the years turn out to be red sensitive like most of the neurons of the turtle retina (6,7,21). The A28 cell was very sensitive to light, saturating at log relative intensities of around -4 (Fig. 5d). At highest intensity, the sustained depolarization lasted considerably longer than the duration of the light flash (lowest trace in Fig. 5d).

Intracellular recordings from another A28 cell recorded in the eyecup preparation revealed essentially the same physiology (Fig. 6). The cell gave a sustained depolarizing response that increased in amplitude with increasing spot diameter (Fig. 6a). At the smallest spot size and highest light intensity, the immediate depolarization was quite transient. At light OFF, especially with medium intensities, small, long-lasting hyperpolarization was typical (Fig. 6a). The receptive field center diameter was larger than the dendritic field size (drawing of cell not shown). Stimulation with large annuli produced definite surround antagonism (Fig. 6a, lower traces show the response is now a sustained hyperpolarization). Like the other two A28s recorded (Fig. 5 and Ammermüller and Kolb [6]) the cell was not color-opponent, the waveforms being the same for all three wavelengths of light stimuli (Fig. 6b).

Table 1 Summary of synaptic input and output to/from the reconstructed turtle Toh-IR cell Present study's data, upper value. Pollard and Eldred's data, lower value.

Types	Number	Strata	% Total
INPUT			
Bipolar Cells	14 3	1, 2/3, 4/5 4/5	5% 20%
Amacrine Cells (some GABA-IR)	209 12	1-5 1, 3, 4/5	95% 80%
OUTPUT			
Amacrine Cells (some GABA-IR)	63 78	mostly in 1 mostly in 1	60% 95%
Ganglion Cells	30 4	1, 2/3, 4/5 1, 4/5	30% 5%
Bipolar Cells	2 0	1	1%
Other Toh-IR Cells	>10 0	mostly in 1	9%
Total Synapses	330 107		

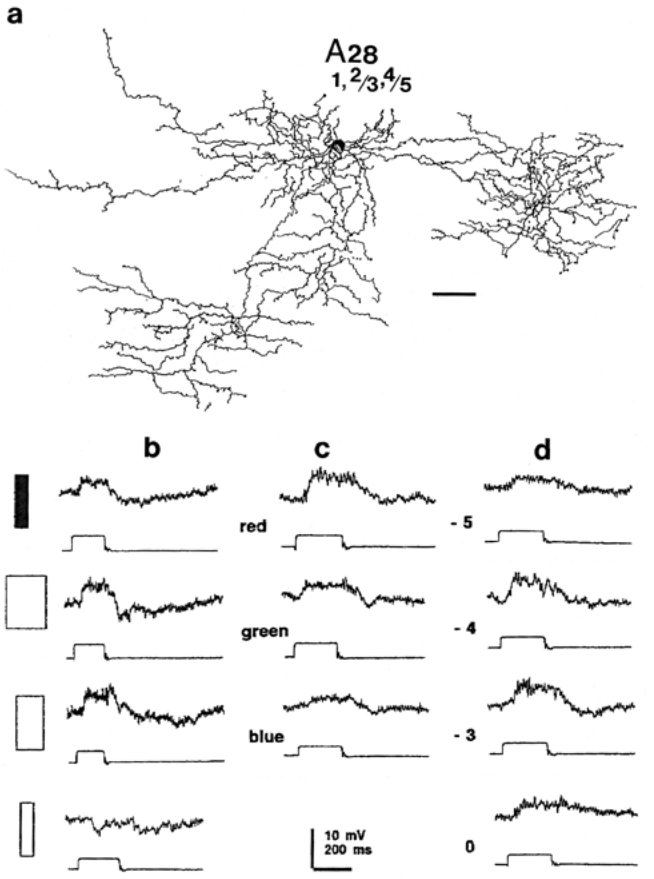

Figure 5. Light reponses of A28 cell. **a)** Camera lucida drawing of an intracellularly recorded and HRP labeled A28 reconstructed from the slice stain. Scale bar 50 µm. **b)** Light responses of the cell as revealed by intracellular recording and staining in the slice preparation. Responses to slits of various widths (from top to bottom: 0.025 mm; 0.45 mm and 0.66 mm slit width) and a black bar (0.15 mm width) surrounded by light. Log. rel. int. = -2. **c)** Responses to 621 nm (red), 505 nm (green) and 404 nm (blue) monochromatic slits (0.45 mm width; 2.3 x 10^8 Quanta/sec/cm^2). **d)** Responses to 621 nm slit stimuli (0.45 mm width) of increasing intensity. Log. relative intensity is indicated by numbers. Full intensity (Log. rel. int. = 0) was 2.3 x 10^{12} Quanta/sec /cm^2.

The cell was quite red-sensitive as most neurons of the turtle retina are (6).

DISCUSSION

In this paper we have studied the morphology, electrophysiology and ultrastructural connectivity of the presumptive dopamine amacrine cell of the turtle retina. The dopamine cell is the tristratified A28 amacrine cell described before for turtle retina (1-4) and proves to be a sustained depolarizing cell with response characteristics dependent on light levels of stimulation. Its synaptic circuitry indicates it to be essentially an interamacrine cell, often with GABAergic cells being the amacrines involved.

Our findings differ somewhat from those of the previous EM study of a Toh-IR cell in turtle retina by Pollard and Eldred (1) (Table 1). We were able to see many more synapses, calculate different percentages to the inputs and outputs, and qualitate the types of synapses with postembedding immunocytochemistry. A notable and important difference between our and their study was the bipolar circuitry associated with A28 cells. We found bipolar axons of strata 1, the 2/3 border, and the 4/5 border to make synaptic contacts and receive reciprocal synapses from the dopamine cell, whereas the other study did not detect these. The bipolar inputs are important in respect to dopamine effects on bipolar cells and sites of dopamine receptors (discussed in a later section). However, despite finding more specific bipolar inputs, we found, in general, bipolar inputs to be far less in number compared to amacrine inputs, a finding that contrasts

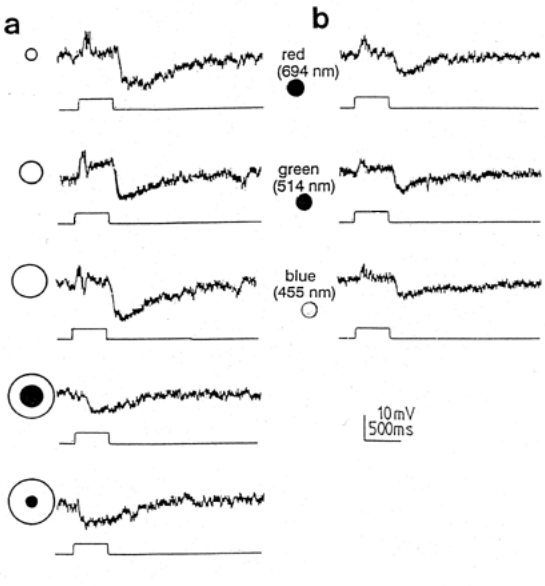

Figure 6. Light response of another A28 cell recorded in the eyecup preparation. **a)** The largest depolarizing transient rides on the depolarizing response to the smallest spot stimulation (660 µm). Increasing the spot size (from top to bottom, 660 µm, 1300 µm and 2000 µm) make the depolarizations smoother and more sustained. An after hyperpolarization is present with small spot stimulation and turns into the sustained surround response after stimulation with the two large annuli (3.2 mm/1,4 mm and 3.2 mm/0.9 mm o.d./i.d.). Light intensity = 1.6 x 10^9 Quanta/sec/cm^2. **b)** Red, green and blue spot stimulation (600 µm dia., wavelengths shown) elicit the same sustained depolarizing responses.

significantly with Pollard and Eldred's study (1). Our dopamine cells were heavily innervated by amacrine cells, many of which are probably GABAergic (Table 1). Our findings suggest that dopamine cells in turtle are essentially controlled by amacrine circuits interposed between bipolar and dopamine cells. A further difference between the two studies is our dopamine cells' greater output to ganglion cells in all three strata in the IPL (Table 1).

Light responses of presumptive turtle dopamine cells—Intracellular recordings of three A28 cells, which are presumptive dopamine cells in turtle retina, have yielded consistent results. Thus all three cells give similar slow, depolarizing responses to light, with slow hyperpolarizations following the OFF of the light stimulus. At high light intensity stimulation, small depolarizing transients occur on the sustained response, and an antagonistic surround is evident.

Recent evidence in the literature increasingly suggests that dopamine cells in vertebrate retinas are depolarizing response types (15-17). This, despite the fact that the vast proportion of dopamine cells in vertebrate retinas have the bulk of their dendrites running in the OFF-center sublamina (sublamina a) of the IPL where they would receive putative hyperpolarizing (OFF-center) bipolar cell inputs. The turtle cell would be no exception concerning this presumed bipolar input, as no depolarizing (ON-center) bipolar cell has yet been seen branching in sublamina **a** in this species (6). However, all evidence points to sign-inverting amacrine inputs being more responsible for dopamine cell response patterns, in turtle at least, than bipolar inputs (8).

Architecture of the dopamine amacrine cell in the turtle retina—Recent reports on intracellular recordings and dye marking of the neurons that contribute to the IPL of the turtle retina (6, 7, 18) have given us insights into the response characteristics of neurons that are likely to be involved with the dopamine amacrine cell. These findings, taken together with other electrophysiological, morphological and neurochemical identifications of neural subtypes in the turtle retina (for reviews: 19-21) allow us to draw a putative wiring diagram of the turtle dopamine system. It is shown in Figure 7A.

There are 6 possible bipolar cells that could have synaptic input to turtle dopamine amacrine cells, three of which are ON-center (center-depolarizing) types physiologically, and three are OFF-center (center hyperpolarizing) types (6,22). B4 and B9 are OFF-center cells but the most attractive candidates for bipolar inputs because they have precise costratification with the dopamine cell (Fig. 7A). B7 is the only center depolarizing candidate (Fig. 7A). B9 is known to be a serotonin-containing bipolar cell (9,23,24). Presumably the small amount of hyperpolarizing B4 or B9 bipolar input compared with amacrine cell inputs cannot as yet be detected in our intracellular recordings.

There are several candidate amacrine cell types having input to the dopamine cell, for 36 different amacrine cell types have been described in turtle retina so far (6). There are particularly large numbers of monostratified types, with sustained hyperpolarizing response characteristics, that run in stratum 1 amongst the main Toh-IR dendritic plexus (6, 21). We suggest that the candidate input amacrines are mainly

hyperpolarizing sustained types because the dopamine amacrine cell is a sustained depolarizing cell, and presumably receives sign-inverting sustained amacrine cell input (black cells in Figure 7A). A12 is the most likely hyperpolarizing amacrine candidate of all, because of its complete dendritic tree overlap with that of the Toh-IR cell. It is a putative glucagonergic cell, a subpopulation of which also contains GABA as a neurotransmitter (25, 26).

There are also candidate sustained, depolarizing amacrine cells that could synapse on the Toh-IR amacrine cell (gray cells in Fig. 7A) to play a role in forming the surround that was seen in the A28 cell's physiological responses. Of these, A15 is bistratified to match two dendritic levels of the Toh-IR cell (Fig. 7A). It is also a putative serotonergic cell, thought possibly to synapse upon the dopamine amacrine cell (9), and our EM findings did reveal there to be a number of synapses from amacrine cell types that contained dense-cored vesicles typical of serotonergic amacrines.

There are two transient ON-OFF amacrine cells that have exact co-stratification with the stratum 2/3 border tier of the Toh-IR cells dendrites (Fig. 7A, A2, A34). We include them as possible candidates for synaptic input responsible for the transients on the initial depolarizing response of A28 to intense light stimulation.

In this study, we saw clear evidence of Toh-IR processes making synapses upon ganglion cell dendrites. This correlates well with Liu and Lasater's study (10) where they found two sorts of responses to dopamine in isolated turtle ganglion cells. Both effects were upon voltage dependent Ca^{++} channels through the D1-cAMP-PKA pathway. But in some ganglion cell types, dopamine application reduced the sustained Ca^{++} currents while in others it facilitated it. It is tempting to suggest that ON-center and OFF-center ganglion cells form the two populations as in other vertebrate retinas (27-32): cells like G19 and G18/G20 respectively (Fig. 7A). Many other turtle ganglion cell types could be postsynaptic candidates as well, of course. However, cells G18, G19 and G20, are most likely equivalent to Liu and Lasater's (10) cells based on cell body measurement.

G20 and G18 are sustained OFF-center types while G19 is a transient ON-center type (6, 7). Smaller-body ganglion cells that may have been missed in the isolated cell studies (10) could obviously also be candidates for dopaminergic amacrine input: G11 can be particularly selected because of its exact costratification with the Toh-IR cell (Fig. 7A).

Role of the dopamine amacrine cell in the circuitry of the IPL— Critz and Marc (8) found that glutamate antagonists that block center-hyperpolarizing bipolar cells produce dopamine release in the turtle retina. They surmised that the effect of the hyperpolarizing bipolars on the dopamine cell was through an intermediary GABAergic amacrine cell because of the effects of bicuculline on dopamine release. The present study has shown that GABA-IR amacrine cells have direct synapses upon Toh-IR cell dendrites, confirming similar contacts that have been seen in other vertebrate retinas (fish, 33; cat, 34). Thus in figure 7B we show the circuit involving hyperpolarizing bipolar (black cell) input to both the dopamine amacrine and a hyperpolarizing sustained GABAergic amacrine, which in turn has inhibitory (sign-inverting synapses) upon the dopamine amacrine. We presume, as suggested by Critz and Marc's data, that the action of GABA is at GABA-A receptors on the dopamine amacrine cell body and dendrites (Fig. 7B). The serotonergic B9 cell (9, 23, 24, 35) is probably the hyperpolarizing bipolar involved (6) and may partially explain the reported interactions between serotonin and dopamine systems in the turtle retina (36). The GABAergic amacrine cell could be the A12 (colocalizing with glucagon, 25,26).

We also show in this study that Toh-IR dendrites made synapses upon ON-center bipolar cells. Thus, the pathway Maguire and Werblin (37) and Wellis and Werblin (38) have recently described in tiger salamander retina, where dopamine modulates the GABA-C receptors mediating inhibition of transmitter release from ON bipolar cells (B7 types) could be

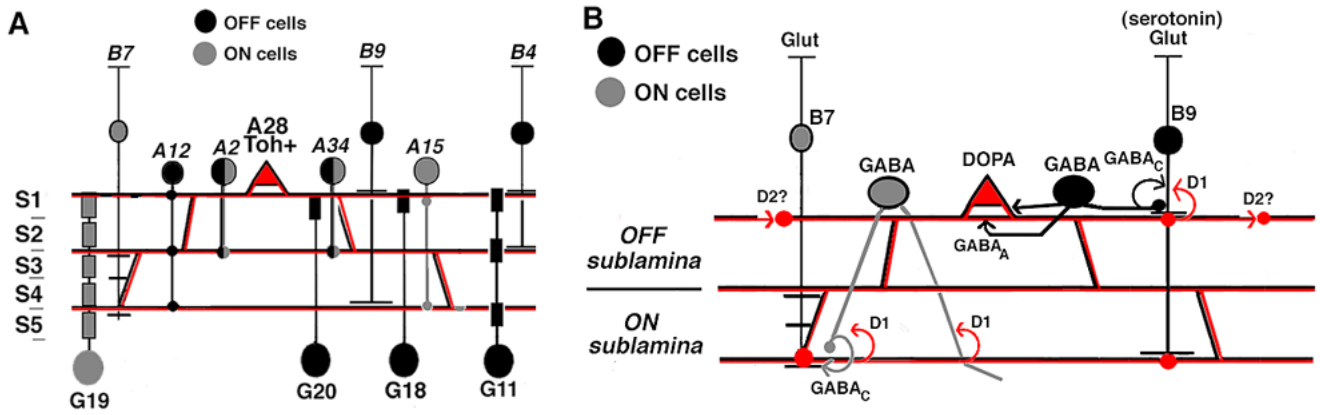

Figure 7. **a)** Wiring diagram of the possible input and output neurons that the dopamine amacrine cell (Toh-IR, A28) is most likely involved with in the IPL of the turtle retina. The tristratified Toh-IR cell (red) is probably driven primarily by B4 and B9 bipolar cells and amacrine cells A12 and A15 because of complete costratification of their processes although all other amacrine and bipolar types could also be involved in a more minor role. The Toh-IR cell most likely synapses upon ganglion cells G11, G18, G19 and G20 for reasons described in the text. The five strata of the IPL are indicated and the center response sign of the various candidate cells are also indicated as black for OFF-center, gray for ON-center and black/gray for ON-OFF cells. **b)** Putative synaptic pathway, neurotransmitter systems (DOPA, Glut, serotonin, GABA) and receptor types (GABAc, GABAc D1 and D2) that could be influencing the response characteristics of the dopamine amacrine (DOPA, red cell). See text for a more detailed explanation.

a possibility in turtle as well (illustrated to right in figure 7B).

Our EM study also showed there to be bipolar input to the dopamine amacrine in the ON sublamina, and furthermore, postsynaptic GABA amacrine profiles were evident here (Fig. 7B, gray profiles). Since recent evidence suggests that dopamine has a similar effect upon ON-center bipolar cells as upon OFF-center bipolar cells in submammalian retinas (38), we suggest a circuit, again through a D1 receptor system, via a depolarizing bipolar (possibly B7) and GABAergic amacrine cells (Fig. 7B, B7, gray cell).

The final circuit that we consider (Fig. 7B) is one where the dopamine cells are communicating in some way, either to enhance or restrict the receptive field organization of the dopamine cell itself. It is possible that dopamine-to-dopamine amacrine cell inhibition via D2 receptors occurs for receptive field surround generation, and that GABAergic disinhibition through the ON center amacrine loop (Fig. 7B) allows the prolonged depolarization after intense light stimulation for the receptive field center that we noted in the physiological experiments.

ACKNOWLEDGEMENTS

Thorsten Meyer recorded the cell in the slice preparation. Laura DeKorver cut the EM serial sections. This research was supported by NIH grant EY04855, Research to Prevent Blindness Corp. and Fight for Sight (EN).

REFERENCES

1. Pollard, J. & Eldred, W.D. (1990). Synaptic analysis of amacrine cells in the turtle retina which contain tyrosine hydroxylase-like immunoreactivity. J. Neurocytol. 19, 53-66.
2. Kolb, H., Cline, C., Wang, H. H. & Brecha, N. (1987). Distribution and morphology of dopaminergic amacrine cells in the retina of the turtle (Pseudemys scripta elegans). J. Neurocytol. 16, 577-588.
3. Nguyen-Legros, J., Versaux-Botteri, C., Vigny, A. & Raoux, N. (1985). Tyrosine hydroxylase immunohistochemistry fails to demonstrate dopaminergic interplexiform cells in the turtle retina. Brain Res. 339, 323-328.
4. Witkovsky, P., Eldred, W. & Karten, H. J. (1984). Catecholamine- and indoleamine-containing neurons in the turtle retina. J.Comp. Neurol. 228, 217-225.
5. Kolb, H., Perlman, I. & Normann, R. A. (1988). Neural organization of the turtle Mauremys caspica. Vis.Neurosci 1, 47-72.
6. Ammermüller, J. & Kolb, H. (1995). The organization of the turtle inner retina I. On- and off-center pathways. J. Comp. Neurol. 358, 1-34.
7. Ammermüller, J., Muller, J. & Kolb, H. (1995). The organization of the turtle inner retina. II. Analysis of color-coded and directionally selective cells. J. Comp. Neurol. 358, 35-62.
8. Critz, S.T. & Marc, R.E. (1992). Glutamate antagonists that block hyperpolarizing bipolar cells increase the release of dopamine from turtle retina. Vis.Neurosci. 9, 271-278.
9. Hurd, L.B. & Eldred, W.D. (1993). Synaptic microcircuitry of bipolar and amacrine cells with serotonin-like immunoreactivity in the retina of the turtle Pseudemys scripta elegans. Vis. Neurosci . 10, 455-472.
10. Liu, Y. & Lasater, E.M. (1994). Calcium currents in turtle retinal ganglion cells II. Dopamine modulation via a cyclic AMP-dependent mechanism. J. Neurophys. 71, 743-752.
11. Eldred, W. D., Zucker, C., Karten, H. J. & Yazulla, S. (1983). Comparison of fixation and penetration enhancement techniques for use in ultrastructural immunocytochemistry. J. Histochem. Cytochem. 31, 285-292.
12. Burkhardt D.A., Gottesman J. & Thoreson W.B. (1989) An eyecup-slice-preparation for intracellular recording in vertebrate retinas. J. Neurosc. Meth.28, 179-187.
13. Dacey, D.M. (1990) The dopaminergic amacrine cell. J. Comp. Neurol. 301, 461-489.
14. Kolb, H., Cuenca, N., Wang, H.-H. & DeKorver, L. (1990). The synaptic organization of the dopaminergic amacrine cell in the cat retina. J. Neurocytol. 19, 343-366.
15. Hashimoto, Y., Abe, M. & Inokuchi, M. (1980) Identification of the interplexiform cell in the dace retina by dye injection method. Brain Res. 197, 331-340.
16. Djamgoz, M.B.A., Usai, C. & Vallerga, S. (1991) An interplexiform cell in the goldfish retina: Light-evoked response pattern and intracellular staining with horseradish peroxidase. Cell Tiss. Res.264, 111-116.
17. Yang, C.-Y., Lukasiewicz, P., Maguire, G., Werblin, F.S. & Yazulla, S. (1991) Amacrine cells in the Tiger salamander retina: Morphology, physiology, and neurotransmitter identification. J. Comp. Neurol. 312, 19-32.
18. Kittila, C. A. & Granda, A. M. (1994). Functional morphologies of retinal ganglion cells in the turtle. J. Comp. Neurol. 350, 623-645.
19. Weiler, R., Ball, A.K. & Ammermüller, J. (1991). Neurotransmitter systems in the turtle retina. Prog. Ret. Res. 10, 1-26.
20. Witkovsky, P. & Dearry, A. (1991). Functional roles of dopamine in the vertebrate retina. Prog. Ret. Res. 11, 247-292.
21. Ammermüller, J. & Kolb, H. (1996) Functional architecture of the turtle retina. Prog. Ret. & Eye Res. 15, 393-433.
22. Marchiafava, P L. & Weiler, R. (1980). Intracellular analysis and structural correlates of the organization of inputs to ganglion cells in the retina of the turtle. Proc. R. Soc. (Lond.) B 208, 103-113.
23. Schutte, M. & Weiler, R. (1987). Morphometric analysis of serotonergic bipolar cells in the retina and its implication for retinal image processing. J. Comp. Neurol. 260, 619-626.
24. Tauchi, M. (1990). Single cell shape and population densities of indoleamine-accumulating and displaced bipolar cells in Reeves' turtle. Proc. R. Soc. (Lond.) B 238, 351-367.
25. Zhang, D. & Eldred, W.D. (1992) Colocalization of enkephalin-, glucagon- and corticotropin releasing factor-like immunoreactivity in GABAergic amacrine cells in turtle retina. Brain Res. 596, 46-57.
26. Eldred, W.D., Ammermüller, J., Schechner, J., Behrens, U.D. & Weiler, R. (1996) Quantitative anatomy, synaptic connectivity and physiology of amacrine cells with glucagon-like immunoreactivity in the turtle retina. J. Neurocytol. 25, 347-364.
27. Ikeda, H., Priest, T.D., Robbins, J. & Wakakuwa, K. (1986). Silent dopaminergic synapses at feline retinal ganglion cells? Clin. Vis. Res. 1, 25-38.
28. Jensen, R.J. (1989). Mechanisms and site of action of dopamine D1 antagonists in the rabbit retina. Vis. Neurosci. 3, 573-581.
29. Jensen, R.J. & Daw, N.W. (1984). Effects of dopamine antagonists on receptive fields of brisk cells and directionally selective cells in the rabbit retina. J. Neurosci. 4, 2972-2985.
30. Jensen, R.J. & Daw, N.W. (1986). Effects of dopamine and its agonists and antagonists on the receptive field properties of ganglion cells in the rabbit retina. Neurosci. 17, 837-855.
31. Straschill, M. & Perwein, J. (1969). The inhibition of retinal ganglion cells by catecholamines and γ-aminobutyric acid. Pflug.Arch. 312, 45-54.
32. Thier, P. & Alder, V. (1984). Action of iontophoretically applied dopamine on cat retinal ganglion cells. Brain Res. 292, 109-121.
33. Yazulla, S. & Zucker, C.L. (1988). Synaptic organization of dopaminergic interplexiform cells in the goldfish retina. Vis. Neurosci. 1, 13-29.
34. Kolb, H., Cuenca, N. & DeKorver, L. (1991). Postembedding immunocytochemistry for GABA and glycine reveals the synaptic relationships of the dopaminergic amacrine cell of the cat retina. J. Comp. Neurol. 310, 267-284.